A glucagon-like peptide-1 analog, liraglutide, ameliorates endothelial dysfunction through miRNAs to inhibit apoptosis in rats

Qian Zhang, Xinhua Xiao, Jia Zheng and Ming Li

Key Laboratory of Endocrinology, Ministry of Health, Department of Endocrinology, Peking Union Medical College Hospital, Peking Union Medical College, Chinese Academy of Medical Sciences, Beijing, China

ABSTRACT

Background and Aims: Many studies have revealed that glucagon-like peptide-1 has vasoprotective effects. In this study, we investigated whether liraglutide suppressed endothelial dysfunction and explored the mechanism involved.

Methods: Experimental diabetes was induced through combined high-fat diet administration and intraperitoneal streptozotocin injections. Rats were randomly divided into the following four groups: control, diabetes, diabetes + a low liraglutide dose (0.2 mg/kg/d), and diabetes + a high liraglutide dose (0.4 mg/kg/d). Endothelial function and metabolic parameters were measured after 8 weeks of treatment. miRNA arrays were analyzed to identify the differentially expressed miRNAs.

Results: We found that liraglutide significantly improved aortic endothelial function in diabetic rats. Liraglutide inhibited miR-93-5p, miR-181a-5p and miR-34a-5p expression, and activated miR-26a-5p expression. miRNA mimic transfection experiments indicated negative relationships between miR-93-5p, miR-181a-5p, miR-34a-5p, and miR-26a-5p and Sirt1, Creb, Bcl-2, and Pten expression, respectively. Moreover, liraglutide increased Sirt1, Creb, and Bcl-2 expression levels and reduced Pten expression level.

Conclusion: Our results demonstrate the role of key miRNAs in the liraglutide-mediated regulation of endothelial cell function in diabetic rats.

Subjects Diabetes and Endocrinology
Keywords Endothelial function, Diabetes, Apoptosis, Liraglutide, miRNA

INTRODUCTION

The worldwide prevalence of diabetes has substantially increased, and diabetes is now recognized as a risk factor for cardiovascular events (*Ogurtsova et al., 2017*). Chronic hyperglycemia induces a high incidence of cardiovascular diseases through several biochemical and physiological pathways (*Capes et al., 2000*). Hence, patients with diabetes have a higher risk of atherosclerotic vascular diseases (*Capes et al., 2000*). Diabetes-induced macrovascular diseases are the leading cause of morbidity and mortality in aging people (*Li et al., 2016*).

Submitted 8 December 2018
Accepted 5 February 2019
Published 6 March 2019

Corresponding author
Xinhua Xiao,
xiaoxh2014@vip.163.com

Academic editor
Paula Moreira

Additional Information and Declarations can be found on page 16

DOI **10.7717/peerj.6567**

MicroRNAs are a series of small non-coding RNAs that are no more than 30 nucleotides long. In most species, the miRNA sequence is perfectly conserved. However, miRNAs have different functions and target different genes in various tissues, species, and physiological conditions. In general, miRNAs bind to the 3′UTR of target genes, thus affecting the post-transcription level of the protein encoded by the gene (*Bartel, 2004*). miRNA is also a primary regulator in the cardiovascular system (*Latronico et al., 2008*; *Quintavalle, Condorelli & Elia, 2011*). The expression levels of some miRNAs, such as miR-126, miR-92a, and miR-21, are specifically increased in vascular endothelial cells. For example, miR-126 regulates the angiogenic ability of endothelial cells (*Fish et al., 2008*; *Wang et al., 2008*), and miR-92a modifies cardiac function in mice with myocardial infarction (*Bonauer et al., 2009*). In smooth muscle cells, miR-21 accelerates cell proliferation through its targets, including tropomyosin 1, phosphatase and tensin homologue on chromosome 10 (*Pten*), and Bcl-2 (*Ji et al., 2007*; *Wang et al., 2011*).

Glucagon-like peptide-1 (GLP-1) is generated from intestinal L-cells that are orally stimulated by glucose loading. GLP-1 participates in glucose-stimulated insulin release and maintains blood glucose homeostasis. However, GLP-1 is rapidly degraded by dipeptidyl peptidase-4 (DPP-4). Since GLP-1 has very short half-life (<2 min after intravenous administration), it is not suitable for a practical option for exogenous therapy (*Plamboeck et al., 2005*). Therefore, liraglutide, a GLP-1 analog, that is, rarely degraded by DPP-4, was approved for diabetes treatment by the US Food and Drug Administration in 2010. Liraglutide is 97% amino acid homology to native GLP-1. The difference between liraglutide and native GLP-1 is acylation of the lysine reside at position 26 with a hexade-canoyl-glutamyl side chain, and a single lysine-to-arginine amino acid substitution at position 34. Like native GLP-1, liraglutide can activate GLP-1 receptor (*Plum, Jensen & Kristensen, 2013*). Meanwhile, liraglutide is non-covalently bound to serum albumin, thus it has decreased rate of elimination (*Malm-Erjefalt et al., 2010*). An increasing amount of evidence shows that GLP-1-based therapies modify cardiovascular function, independent of blood glucose (*Bao et al., 2011*; *Bhashyam et al., 2010*). Endothelial dysfunction plays a key role in the early stage of atherosclerosis in diabetes (*Chakravarthy et al., 1998*). However, little is known regarding liraglutide-induced miRNA actions on endothelial function in diabetic rats.

Thus, in this study, we established a diabetic rat model and applied miRNA microarray and bioinformatics analysis to determine whether liraglutide attenuates vascular dysfunction through miRNA and to explore the underlying mechanism responsible for these effects.

MATERIALS AND METHODS

Animal treatments and diets

Five-week-old male Sprague–Dawley rats (150–180 g) were purchased from the Institute of Laboratory Animal Science, Chinese Academy of Medical Sciences, and Peking Union Medical College (SCXK-2014-0013; Beijing, China). All procedures were performed in accordance with the Guide for the Care and Use of Laboratory Animals published by the US National Institutes of Health (NIH publication No. 85-23, revised 1996) and were

approved by the Animal Care Committee of the Peking Union Medical Hospital Animal Ethics Committee (Project XHDW-2015-0051, February 15, 2015). All efforts were made to minimize suffering, and all rats were housed in an environment with controlled temperature (21–23 °C), humidity (50–60%), and light-dark (12:12 h) cycle. After a 1-week acclimatization period, a normal diet (% kcal: 10% fat, 20% protein, and 70% carbohydrate; 3.85 kcal/g) was provided to normal control rats (n = 6), and a high-fat diet (% kcal: 45% fat, 20% protein, and 35% carbohydrate; 4.73 kcal/g, Research Diet, New Brunswick, NJ, USA) was provided to the other rats (n = 18). After 4 weeks, rats fed the high-fat diet were intraperitoneally injected with streptozotocin (STZ, 30 mg/kg body weight) to develop the induced type 2 diabetes rodent model (*Skovso, 2014*). The diabetes model was considered successful when rats had fasting blood glucose (FBG) levels exceeding 11.1 mmol/L. Then, diabetic rats were randomly divided into the following three groups (n = 6 per group): diabetes + vehicle group (DM, n = 6), low liraglutide dose (LL, n = 6), and high liraglutide dose (HL, n = 6). According previous reports (*Hoang et al., 2015*; *Yang et al., 2018*), LL and HL groups were treated with liraglutide at 0.2 and 0.4 mg/kg/d by daily subcutaneous injections for 12 weeks, respectively. Liraglutide doses were based on human dosages adjusted for rodent body weight (*Larsen et al., 2008*; *Sturis et al., 2003*). The diabetes + vehicle and control groups were injected with the same volume of normal saline. In addition, the DM, LL, and HL groups were maintained on the high-fat diet through the end of the experiment. At the end of the experiment, the rats were fasted overnight and then anesthetized. Blood samples were obtained from the abdominal aorta. Then, the rats were sacrificed by decapitation. Thoracic aortas were quickly removed, and some of the thoracic aortas were placed in Krebs solution (120 mmol/L NaCl, 4.7 mmol/L KCl, 1.18 mmol/L KH_2PO_4, 2.25 mmol/L $CaCl_2$, 24.5 mmol/L $NaHCO_3$, 1.2 mmol/L $MgSO_4{\cdot}7H_2O$, 11.1 mmol/L glucose, 0.03 mmol/L EDTA) that was aerated with 95% O_2 and 5% CO_2. The aortas were cut into three-mm-long rings for vascular reactivity assays. The remaining aortas were frozen in liquid nitrogen and stored at −80 °C for miRNA arrays and quantitative PCR assays.

Oral glucose tolerance test

Rats were fasted overnight and were then administered glucose (two g/kg) by gavage (*Andrikopoulos et al., 2008*; *Islam et al., 2009*). After glucose loading, blood samples were collected from the tail at 30, 60, and 120 min. Blood glucose levels were measured by a Bayer Contour TS Glucometer (Hamburg, Germany). The blood glucose area under the curve (AUC) was calculated by the linear trapezoid method (*Zhang et al., 2016*).

Measurement of fasting serum insulin and homeostasis model assessment of insulin resistance

Serum insulin was determined by ELISA (Millipore, Bellerica, MA, USA). To assess insulin resistance status, homeostasis model assessment of insulin resistance (HOMA-IR) was calculated by FBG (mmol/L) × fasting serum insulin (μIU/mL)/22.5 (*Antunes et al., 2016*).

Vascular reactivity assay

Vascular reactivity was measured as described previously (*Matsumoto et al., 2014*). Thoracic aortas were cut into three-mm rings in Krebs solution aerated with 95% O_2 and 5% CO_2 at 37 °C. The rings were pre-contracted with phenylephrine to produce maximal contraction. Then, increasing concentrations of acetylcholine (ACh) were added to the solution to obtain a cumulative concentration-response curve. Isometric tension was recorded using on a BL-410 biological function system (Chengdu Tai Meng Science and Technology Co., Ltd., Chengdu, China).

RNA extraction and microarray hybridization

To identify key miRNAs modified by liraglutide, we analyzed miRNA microarrays with aorta RNA from the DM and HL groups. RNA from the aorta was extracted using a mirVana^{TM} RNA Isolation Kit (Ambion, Sao Paulo, SP, Brazil). High quality RNA was reverse transcribed into cDNA. cRNA followed by double-stranded cDNA were produced. cDNA was labeled by biotin, and then hybridized to an Affymetrix Multispecies miRNA 4.0 array (Affymetrix Technologies, Santa Clara, CA, USA). Data normalization and analysis were performed with Expression Console software (version 1.4.1, Affymetrix Technologies, Santa Clara, CA, USA). Calculated *P*-values were based on Student's *t*-tests. miRNAs with fold changes >1.5 and *P*-values < 0.05 were considered differentially expressed miRNAs. A heat map of differentially expressed miRNAs was drawn by using TIGR MeV (MultiExperiment Viewer) software (http://mev.tm4.org/) (*Saeed et al., 2006*). The microarray raw data were submitted to the Gene Expression Omnibus repository (GSE102198). The validated targets of differentially expressed miRNAs were searched in miRTarBase database version 6.0 (http://mirtarbase.mbc.nctu.edu.tw/, released September 2015) (*Chou et al., 2016*).

qRT-PCR for miRNA expression analysis

RNA was isolated as previously described. Reverse transcription was performed by using a miScript^{TM} reverse transcription kit (Qiagen, Hilden, Germany). For miRNA expression, qRT-PCR was performed by using a TaqMan PCR kit (Applied Biosystems, Foster City, CA, USA) and an ABI 7700 system (Applied Biosystems, Foster City, CA, USA). The reaction conditions were as follows: 10 min at 95 °C, followed by 45 cycles of 15 s at 95 °C, and 60 s at 60 °C. miRNA expression levels were normalized to U6 expression.

qRT-PCR for target gene analysis

qRT-PCR for target genes was performed by using a SYBR Green kit (Applied Biosystems, Foster City, CA, USA). PCR was carried out on an ABI 7700 system (Applied Biosystems, Foster City, CA, USA) using the following reaction conditions: 15 min at 95 °C, followed by 40 cycles of 15 s at 95 °C and 60 s at 64 °C. All gene expression levels were normalized to CypA (cytochrome P450 A) expression. The primers are listed in Table 1.

Table 1 Oligonucleotide sequences for qPCR analysis.

Gene symbol	Genebank ID	Forward primer	Reverse primer	Annealing temperature (°C)	Product size
Bcl2	NM_016993	GGGATGACTTCTCTCGTCGC	TGACATCTCCCTGTTGACGC	65	200
Creb1	NM_031017	GCAGTGACTGAGGAGCTTGT	TGAGCTGCTGGCATGGATAC	65	169
Pten	NM_031606	CCAGTCAGAGGCGCTATGTA	TCCGCCACTGAACATTGGAA	64	122
Sirt1	XM_017601788	AAGGCAGACAATTTAATGGGGT	ATCGAACATGGCTTGAGGATCT	64	150

Note:
Creb1, cAMP responsive element binding protein 1; *Pten*, phosphatase and tensin homolog; *Sirt1*, sirtuin.

Western blotting

Aorta were homogenized in RIPA buffer. Denatured protein (50 μg) were separated on 10% sodium dodecyl sulfate polyacrylamide gel electrophoresis. Polyvinylidene difluoride membranes (Bio-Rad, Hercules, CA, USA) were blocked in Tris-buffered saline buffer with skimmed milk for 30 min, followed by overnight incubation at 4 °C with rabbit anti-PTEN (1:1,000, Cell Signaling Technology, Danvers, MA, USA) or mouse anti-Bcl-2 (1:1,000, Abcam, Cambridge, UK). After washing, membranes were incubated with horseradish peroxidase conjugated secondary antibody for 2 h at room temperature. After incubation, membranes were washed and developed using a chemiluminescence (ECL, Cell Signaling Technology, Danvers, MA, USA) assay. The housekeeping protein β-actin (1:5,000, Abcam, Cambridge, UK) was used for normalization.

Target gene function and pathway analysis

For miRNA target functional analysis, the database for annotation, visualization, and integrated discovery (DAVID) was used to extract biological features associated with miRNA target gene lists (*Dennis et al., 2003*). The software performed an enrichment analysis of miRNA target genes with all known Gene Ontology (GO) terms and Kyoto Encyclopedia of Genes and Genomes (KEGG) pathways.

Cell culture, treatment, and transfection

Human umbilical vein endothelial cells (HUVECs, Life Technologies, Invitrogen^{TM}, Carlsbad, CA, USA) were cultured in EGM-2 MV BulletKit medium (Lonza Group Ltd., Basel, Switzerland) in a humidified incubator containing 5% CO_2 at 37 °C. Based on the miRNA sequence registered in the miRBase database, miRNA mimics, and negative control oligoduplex (Ambion, Thermo Fisher Scientific Inc., Cambridge, MA, USA) were synthesized. HUVECs were transfected with miRNA mimics (50 nM) or negative control using Lipofectamine RNAiMAX transfection reagent (Life Technologies, Carlsbad, CA, USA) for 48 h.

Data analysis

All data are presented as the mean ± standard deviation (SD). Statistical analysis was determined by Student's *t*-test and one-way ANOVA, followed by the Tukey–Kramer test for post hoc comparisons using GraphPad Prism software (version 5.0, San Diego, CA, USA).

Table 2 Metabolic parameters in four groups after treatment.

Parameters	Groups			
	CON	DM	LL	HL
Body weight (g)	512.0 ± 15.5	499.5 ± 9.5	469.8 ± 10.9$^{*\#}$	467.8 ± 7.3$^{*\#}$
Fasting blood glucose (mmol/L)	5.35 ± 0.41	18.95 ± 2.80**	14.71 ± 2.39$^{**\#\#}$	13.78 ± 2.12$^{**\#\#}$
Fasting serum insulin (ng/mL)	0.89 ± 0.15	1.49 ± 0.33**	0.87 ± 0.21$^{\#}$	0.94 ± 0.19$^{\#}$
HOMA-IR	4.51 ± 1.07	26.59 ± 6.96**	12.30 ± 4.47$^{**\#\#}$	12.37 ± 4.28$^{**\#\#}$
AUCg (mmol/L/h)	15.61 ± 0.86	46.45 ± 4.94**	38.08 ± 1.83$^{**\#\#}$	32.01 ± 3.29$^{**\#\#}$

Notes:
HOMA-IR, homeostasis model assessment of insulin resistance; AUCg, the blood glucose area under the curve; CON, control; DM, diabetes mellitus; LL, low dose of liraglutide; HL, high dose of liraglutide.
Data were presented as mean ± standard deviation (n = 6/group). $^{*}P < 0.05$, $^{**}P < 0.01$, vs CON; $^{\#}P < 0.05$, $^{\#\#}P < 0.01$ vs diabetic.

Table 3 Vasorelaxation responses (%) to ACh of thoracic aortic rings after treatment.

Groups	ACh (mol/L)						
	1×10^{-10}	1×10^{-9}	1×10^{-8}	1×10^{-7}	1×10^{-6}	1×10^{-5}	1×10^{-4}
CON	89.8 ± 1.8	83.4 ± 2.4	70.5 ± 3.6	52.5 ± 5.0	33.3 ± 5.5	20.9 ± 5.2	13.5 ± 5.1
DM	91.1 ± 3.6	83.5 ± 1.1	69.1 ± 4.5	57.7 ± 3.4*	40.5 ± 2.5**	28.7 ± 1.3**	21.2 ± 2.6**
LL	91.0 ± 1.5	83.2 ± 3.6	70.9 ± 3.8	48.4 ± 4.3$^{\#\#}$	33.7 ± 3.6$^{\#\#}$	20.4 ± 2.3$^{\#\#}$	13.1 ± 2.3$^{\#\#}$
HL	89.5 ± 2.6	81.0 ± 2.2	71.9 ± 4.0	49.9 ± 2.4$^{\#\#}$	30.7 ± 2.2$^{\#\#}$	17.8 ± 2.2$^{\#\#}$	11.8 ± 2.4$^{\#\#}$

Notes:
Data were presented as mean ± standard deviation (n = 6). $^{*}P < 0.05$, $^{**}P < 0.01$, vs CON; $^{\#\#}P < 0.01$, vs DM.
CON, control; DM, diabetes mellitus; LL, low dose of liraglutide; HL, high dose of liraglutide.

RESULTS

Effect of liraglutide on metabolic parameters in diabetic rats

Metabolic parameters of the experimental rats are summarized in Table 2. Liraglutide significantly decreased body weight after 12 weeks of treatment ($P < 0.05$). Diabetic rats had significant hyperglycemia and higher AUC value in oral glucose tolerance test (OGTT) than that in normal rats ($P < 0.01$). Both low dosage and high dosage of liraglutide treatment could reduce FBG and AUC level in OGTT ($P < 0.01$). Moreover, diabetic rats had higher fasting serum insulin and HOMA-IR than that in normal rats ($P < 0.01$). Liraglutide reduced fasting serum insulin ($P < 0.05$) and HOMA-IR value ($P < 0.01$).

Effect of liraglutide on endothelial function in diabetic rats

To evaluate the effect of liraglutide on endothelial function in diabetic rats, endothelium-dependent vasodilation was examined. As shown in Table 3, diabetic rats had significantly impaired endothelium-dependent vasodilation in response to ACh, compared with that in normal rats ($P < 0.01$). Liraglutide treatment ameliorated the impairment of endothelium-dependent vasodilation ($P < 0.01$).

miRNA array results

The miRNA expression profiles of the HL and DM groups were identified by miRNA arrays. The results revealed that 33 miRNAs were significantly changed in the HL group

Table 4 Differential expression miRNAs in HL group vs DM group ($P < 0.05$, Fold change >1.5).

miRNA	Fold change	*P*-value	Mature sequence
rno-miR-297	2.817	0.027	AUGUAUGUGUGCAUGUAUGCAUG
rno-miR-592	2.244	0.016	AUUGUGUCAAUAUGCGAUGAUGU
rno-miR-671	2.176	0.020	UCCGGUUCUCAGGGCUCCACC
rno-miR-214-3p	2.129	0.006	ACAGCAGGCACAGACAGGCAG
rno-miR-1843-3p	2.037	0.028	UCUGAUCGUUCACCUCCAUACA
rno-miR-6334	1.991	0.015	CCAGGCUCUCCCAGCUGCCGGC
rno-miR-103-1-5p	1.948	0.023	GGCUUCUUUACAGUGCUGCCUUGU
rno-miR-466b-5p	1.907	0.041	UAUGUGUGUGUGUAUGUCCAUG
rno-miR-96-5p	1.812	0.045	UUUGGCACUAGCACAUUUUUGCU
rno-miR-190a-5p	1.740	0.042	UGAUAUGUUUGAUAUAUUAGGU
rno-let-7c-5p	1.726	0.026	UGAGGUAGUAGGUUGUAUGGUU
rno-mir-22	1.713	0.039	ACCUGGCUGAGCCGCAGUAGUUCUU CAGUGGCAAGCUUUAUGUCCUGA CCCAGCUAAAGCUGCCAGUUGAA GAACUGUUGCCCUCUGCCACUGGC
rno-mir-190a	1.687	0.019	UGCAGGCCUCUGUGUGAUAUGUUU GAUAUAUUAGGUUGUUAUUUAA UCCAACUAUAUAUCAAGCAUAUU CCUACAGUGUCUUGCC
rno-miR-568	1.667	0.001	AUGUAUAAAUGUAUACACAC
rno-miR-3586-3p	1.654	0.037	AUACUAGACUGUGAGCUCCUCGA
rno-miR-675-3p	1.602	0.019	UGUAUGCCCUAACCGCUCAGU
rno-mir-214	1.596	0.005	GUCCUGGAUGGACAGAGUUGUCA UGUGUCUGCCUGUCUACACUUG CUGUGCAGAACAUCCGCUCAC CUGUACAGCAGGCACAGACAGG CAGUCACAUGACAACCCAGCCU
rno-miR-134-5p	1.592	0.015	UGUGACUGGUUGACCAGAGGGG
rno-miR-26a-5p	1.585	0.021	UUCAAGUAAUCCAGGAUAGGCU
rno-miR-488-3p	1.565	0.012	UUGAAAGGCUGUUUCUUGGUC
rno-mir-188	1.513	0.032	CCCUCUCUCACAUCCCUUGCAUGG UGGAGGGCGAGCUCUCUGAAAA CUCCUCCCACAUGCAGGGUUUG CAGGAUGGUGAG
rno-miR-126a-5p	−1.555	0.011	CAUUAUUACUUUUGGUACGCG
rno-miR-181a-5p	−1.597	0.028	AACAUUCAACGCUGUCGGUGAGU
rno-miR-879-5p	−1.639	0.041	AGAGGCUUAUAGCUCUAAGCC
rno-miR-541-3p	−1.668	0.013	AGUGGCGAACACAGAAUCCAUAC
rno-mir-344b-1	−1.729	0.007	AGAGACCUGAUCAGUCAGGCUGC UGGUUAUAUUCCAGGACUUCU CUGGUCCUGGAUAUAACCAAA GCCCGACUGUUAAAUAAAAGU AAGAAUGUGUCU
rno-let-7b-5p	−1.766	0.030	UGAGGUAGUAGGUUGUGUGGUU
rno-miR-3571	−1.837	0.046	UACACACUUCUUUACAUUCCAUA

(Continued)

Table 4 (continued).

miRNA	Fold change	*P*-value	Mature sequence
rno-miR-547-5p	−1.942	0.026	UCACUUCAGGAUGUACCACCCA
rno-miR-349	−1.980	0.007	CAGCCCUGCUGUCUUAACCUCU
rno-miR-544-3p	−1.984	0.044	AUUCUGCAUUUUUAGCAAGCU
rno-miR-34a-5p	−2.079	0.024	UGGCAGUGUCUUAGCUGGUUGU
rno-miR-93-5p	−2.715	0.037	CAAAGUGCUGUUCGUGCAGGUAG

Note:
DM, diabetes mellitus; HL, high dose of liraglutide.

(fold change >1.5, $P < 0.05$, Table 4). Among these 33 miRNAs, 21 miRNAs were upregulated (miR-297, miR-592, miR-671, miR-214-3p, miR-1843-3p, miR-6334, miR-103-1-5p, miR-466b-5p, miR-96-5p, miR-190a-5p, let-7c-5p, mir-22, mir-190a, miR-568, miR-3586-3p, miR-675-3p, mir-214, miR-134-5p, miR-26a-5p, miR-488-3p, mir-188), and 12 miRNAs were downregulated (miR-93-5p, miR-34a-5p, miR-544-3p, miR-349, miR-547-5p, miR-3571, let-7b-5p, mir-344b-1, miR-541-3p, miR-879-5p, miR-181a-5p, miR-126a-5p). Hierarchical clustering of these 33 differentially expressed miRNAs was then performed. Figure 1 shows separate clusters for the diabetes and HL samples.

Assay of four differentially expressed miRNAs in the four groups

In this experiment, we evaluated four differentially expressed miRNAs in the liraglutide-treated group, as these miRNAs were predicted function to be involved in endothelial function. The four differentially expressed miRNAs were quantified by qPCR to validate the results, as shown in Fig. 2. Among these four miRNAs, all were differentially expressed between the diabetes and HL groups ($P < 0.01$). The results agreed with the miRNA array data.

Bioinformatic analysis of the targets of 33 differentially expressed miRNAs

In the miRTarBase database, we found 32 experimentally validated target genes from 11 differentially expressed miRNAs (Table 5). Enrichment analysis of the validated target genes was performed to identify the biological processes relevant to the 11 differentially expressed miRNAs in the HL group. GO and KEGG pathway analyses of the targets were performed by using the DAVID database. The results revealed that the 11 miRNAs were involved in eight physiological processes, including the cellular response to tumor necrosis factor, the positive regulation of endothelial cell chemotaxis to fibroblast growth factor, angiogenesis, branching involved in salivary gland morphogenesis, etc. ($P < 0.05$, Table 6). Table 7 lists the top 10 pathways and relevant target genes that were significantly correlated with the 33 miRNAs ($P < 0.05$). The pathways could contribute to the mechanisms of the PI3K-AKT signaling pathway. Figure 3 shows the miRNA-target gene network. Interestingly, several differentially expressed miRNAs regulate genes in the PI3K-AKT signaling pathway.

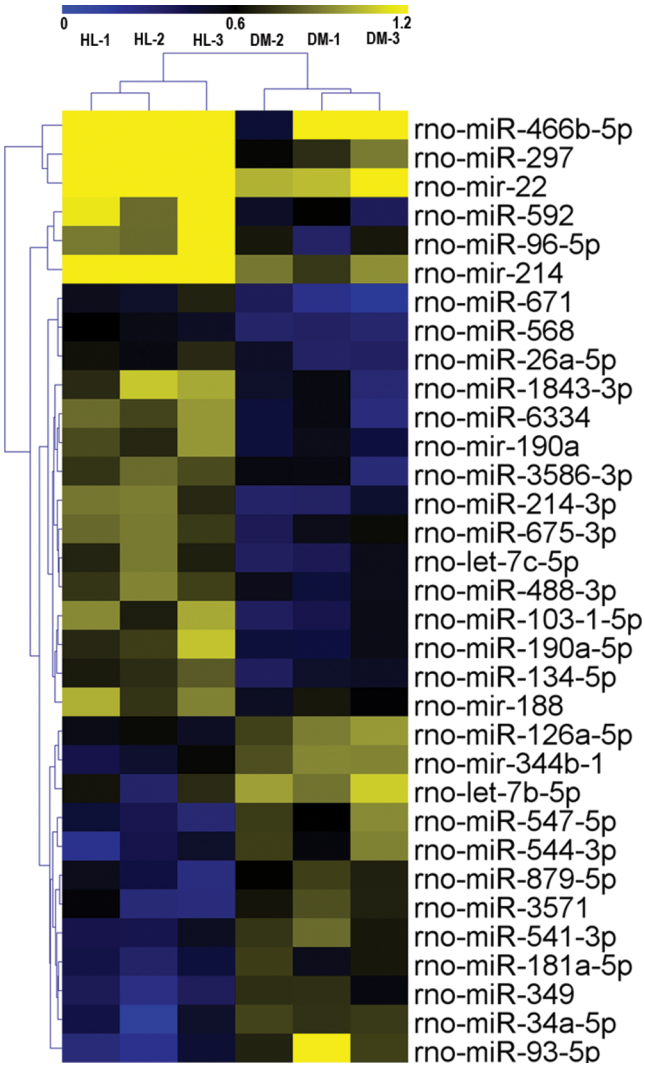

Figure 1 Hierarchical clustering for differentially expressed miRNAs in HL group vs DM group. CON, control; HL, high liraglutide dose. Full-size DOI: 10.7717/peerj.6567/fig-1

Target gene expression in qPCR

We found that *Pten* expression was significantly upregulated ($P < 0.01$, Fig. 4); however, *Creb1*, *Bcl2*, and *Sirt1* levels were significantly downregulated in the DM group ($P < 0.01$, Fig. 4). Liraglutide reduced *Pten* expression and increased *Creb1*, *Bcl2*, and *Sirt1* expression ($P < 0.01$, Fig. 4).

Protein expression in western blot

Total protein expression of PTEN was significantly higher, while Bcl-2 was lower in DM group than that in CON group ($P < 0.01$, Fig. 5). Liraglutide reduced PTEN expression and increased Bcl-2 expression in aorta ($P < 0.01$, Fig. 5).

Target gene expression in miRNA mimic-transfected HUVECs

To determine whether miR-26a-5p, miR-181a-5p, miR-34a-5p, and miR-93-5p negatively regulate their target genes in vitro, HUVECs were transfected with respective miRNA

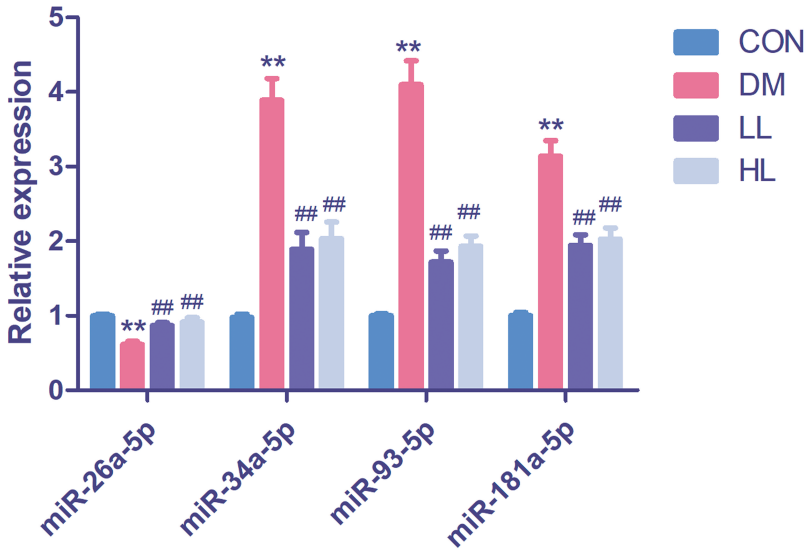

Figure 2 Real time quantification results of the four differentially expressed miRNAs in four groups. Data were presented as mean ± standard deviation (n = 6). CON, control; DM, diabetes; LL, low liraglutide dose; HL, high liraglutide dose. $^{**}P < 0.01$ vs CON group; $^{\#\#}P < 0.01$ vs DM group.
Full-size DOI: 10.7717/peerj.6567/fig-2

Table 5 Validated target for differentially expressed miRNAs.

miRNA	Regulation	Target genes
rno-miR-214-3p	Up	Fgf16, Gpd1, Arl2, Fgfr1, Scn3a
rno-miR-96-5p	Up	Mitf
rno-miR-190a-5p	Up	Ccl2, Neurod1, Pappa
rno-let-7c-5p	Up	Vim
rno-miR-26a-5p	Up	Map2, Pten
rno-miR-134-5p	Up	Bdnf, Limk1, Pum2
rno-miR-126a-5p	Down	Cyp2a3
rno-miR-181a-5p	Down	Gpx1, Gria2, Tgm2, Creb1
rno-let-7b-5p	Down	Tagln, Vim
rno-miR-34a-5p	Down	Bcl2, Sp1, Tagln, Notch1, Grm7, Capn8, Mgst1, E2f3, Mycn, Sirt1
rno-miR-93-5p	Down	Kcnj14, Sp1, Mgst1, Sirt1

mimics. *Pten*, *Creb*, *Bcl-2*, and *Sirt1* expression was significantly reduced in miR-26a-5p, miR-181a-5p, miR-34a-5p, and miR-93-5p mimic transfected HUVECs, respectively ($P < 0.01$, Fig. 6).

DISCUSSION

In our study, we showed that liraglutide treatment significantly ameliorated blood glucose and insulin resistance status in diabetic rats. Then, we used aortic rings to evaluate ACh-induced endothelium-dependent vasodilation. ACh-induced endothelium-dependent vasodilation was impaired in diabetic rats, while liraglutide augmented endothelial function. Clinical trials prove liraglutide as a potent drug for

Table 6 The genes regulated by the 11 miRNAs related to several biology processes ($P < 0.05$).

Term ID	Term name	Count	*P*-value	Genes	Fold enrichment
GO:0071356	Cellular response to tumor necrosis factor	3	0.002362	GPD1, CCL2, SIRT1	39.2
GO:2000546	Positive regulation of endothelial cell chemotaxis to fibroblast growth factor	2	0.005899	FGFR1, FGF16	323.0
GO:0001525	Angiogenesis	3	0.013624	FGFR1, SIRT1, PTEN	15.9
GO:0060445	Branching involved in salivary gland morphogenesis	2	0.017599	FGFR1, TGM2	107.6
GO:0060045	Positive regulation of cardiac muscle cell proliferation	2	0.027248	FGFR1, NOTCH1	69.2
GO:0002053	Positive regulation of mesenchymal cell proliferation	2	0.031083	FGFR1, MYCN	60.5
GO:0048754	Branching morphogenesis of an epithelial tube	2	0.034903	NOTCH1, MYCN	53.8
GO:0030534	Adult behavior	2	0.040606	GRM7, PTEN	46.1

Table 7 The genes regulated by the 11 miRNAs related to several pathways ($P < 0.05$).

Pathway ID	Pathway term	Count	*P*-value	Genes	Fold enrichment
rno05218	Melanoma	5	3.42×10^{-5}	FGFR1, E2F3, MITF, FGF16, PTEN	24.8
rno05215	Prostate cancer	5	7.62×10^{-5}	FGFR1, E2F3, CREB1, BCL2, PTEN	20.2
rno05206	MicroRNAs in cancer	6	1.14×10^{-4}	NOTCH1, E2F3, BCL2, VIM, SIRT1, PTEN	11.3
rno05200	Pathways in cancer	6	0.003477	FGFR1, E2F3, BCL2, MITF, FGF16, PTEN	5.3
rno05161	Hepatitis B	4	0.006636	E2F3, CREB1, BCL2, PTEN	9.7
rno05030	Cocaine addiction	3	0.007296	BDNF, GRIA2, CREB1	22.0
rno05031	Amphetamine addiction	3	0.013088	GRIA2, CREB1, SIRT1	16.2
rno04151	PI3K-Akt signaling pathway	5	0.013482	FGFR1, CREB1, BCL2, FGF16, PTEN	5.0
rno05016	Huntington's disease	4	0.015083	BDNF, SP1, CREB1, TGM2	7.2
rno05222	Small cell lung cancer	3	0.023206	E2F3, BCL2, PTEN	12.0

diabetic patients with cardiovascular disease. The Liraglutide Effect and Action in Diabetes: Evaluation of Cardiovascular Outcome Results trial showed that patients treated with liraglutide had fewer primary outcomes pertaining to non-inferiority, cardiovascular-related death, or all-cause death than patients treated with a placebo (*Marso et al., 2016*). Many in vitro and in vivo animal research proves the benefit of liraglutide on vascular. In rat branched mesenteric arteries, liraglutide induce significant relaxation compared with vehicle (*Bangshaab et al., 2018*). In rodent research, liraglutide also inhibits endothelial cell dysfunction in $ApoE^{-/-}$ mouse model (*Gaspari et al., 2011*).

A previous study indicated the synergistic effect of liraglutide with metformin on endothelial dysfunction through the GLP-1 receptor and the protein kinase A signaling pathway (*Ke et al., 2017*). In our study, pathway analysis revealed many miRNA targets in the PI3K-AKT pathway. The PI3K-AKT signaling pathway plays various roles in cell biology function, including endothelial cell proliferation. A previous study revealed that PI3K-AKT signaling inhibited human cardiac microvascular endothelial cells (HCMEC) apoptosis and hypoxia/reoxygenation (HR)-induced endothelial dysfunction. Moreover, the PI3K-AKT pathway prevented HR-induced myocardial microvascular endothelial cell

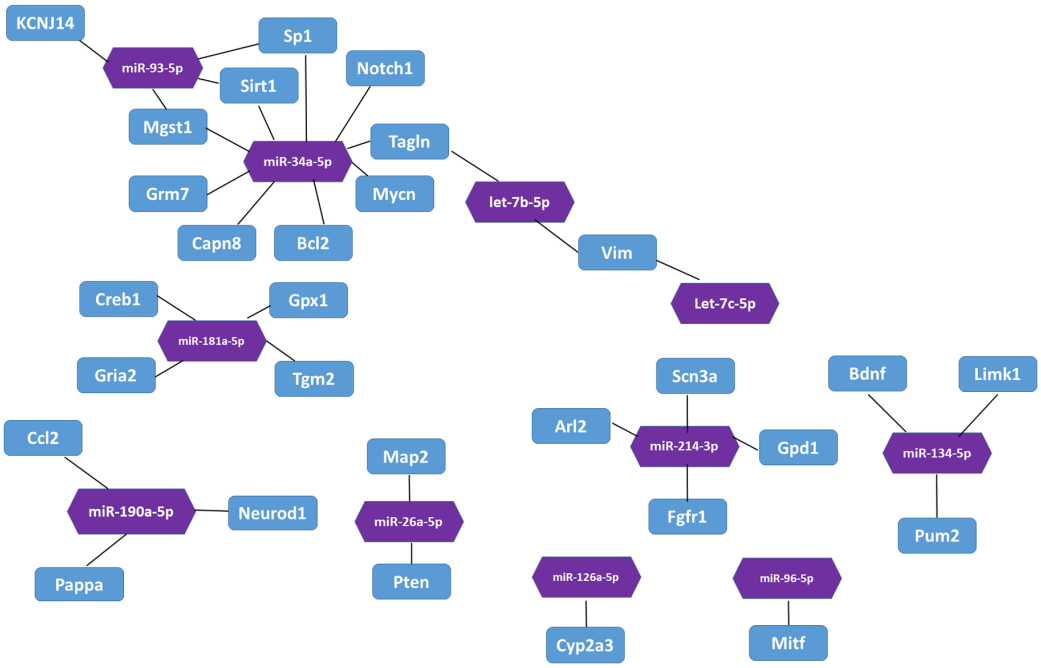

Figure 3 The interaction between miRNA and target genes. Purple hexagon indicates miRNAs and blue rectangles indicates target genes. Full-size DOI: 10.7717/peerj.6567/fig-3

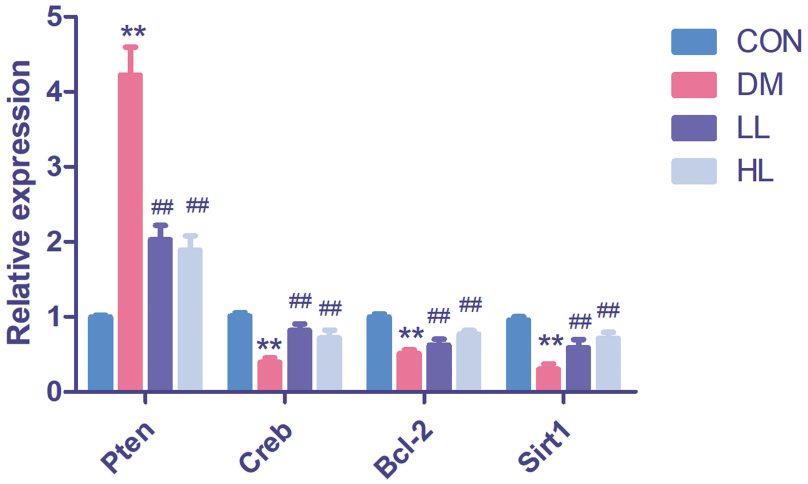

Figure 4 Real time quantification results of the miRNAs target genes in four groups. *Creb1*, cAMP responsive element binding protein 1; *Pten*, phosphatase and tensin homolog; *Sirt1*, sirtuin; CON, control; DM, diabetes; LL, low liraglutide dose; HL, high liraglutide dose. Data were presented as mean ± standard deviation (n = 6). $^{**}P < 0.01$ vs CON group; $^{\#\#}P < 0.01$ vs DM group.
Full-size DOI: 10.7717/peerj.6567/fig-4

apoptosis (*Su et al., 2014*). Increased levels of Bcl-2, PI3K, and phosphorylated AKT can protect HCMECs from HR injury (*Xie et al., 2016*). The liraglutide-treated group presented with increased miR-26a-5p expression. In addition, an in vitro experiment also showed that liraglutide increased miR-26a-5p expression in high glucose-exposed HUVECs. PTEN is a miR-26a-5p target genes that can dephosphorylate

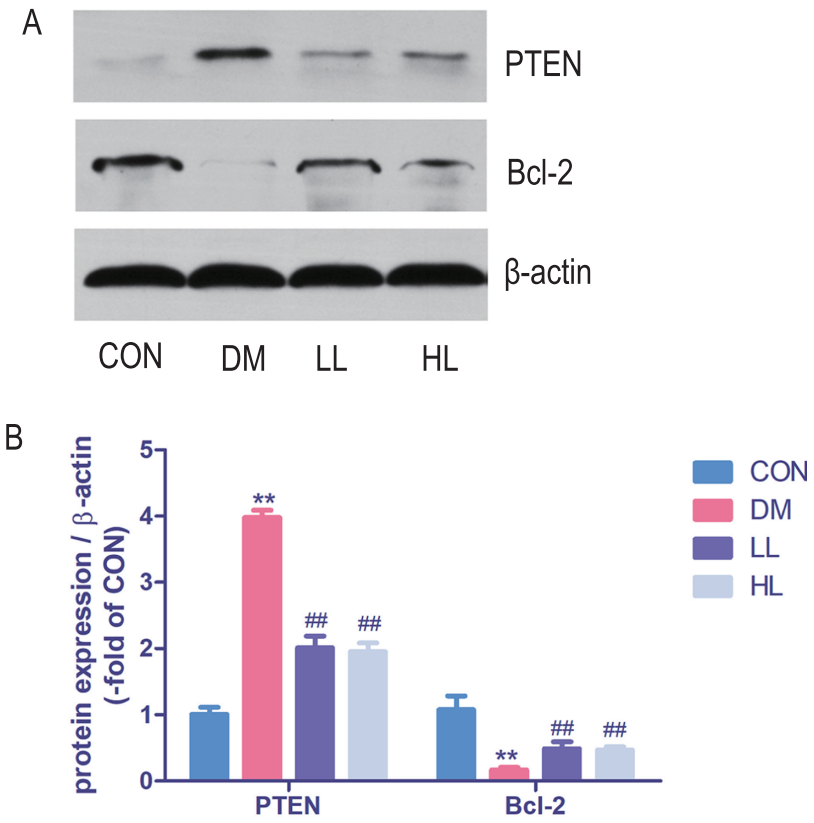

Figure 5 Protein expression levels were detected by Western blot. CON, control; DM, diabetes; LL, low liraglutide dose; HL, high liraglutide dose; PTEN, phosphatase and tensin homolog. Data were presented as mean ± standard deviation ($n = 6$). $^{**}P < 0.01$ vs CON group; $^{\#\#}P < 0.01$ vs DM group.
Full-size DOI: 10.7717/peerj.6567/fig-5

phosphatidylinositol-3,4,5-triphosphate produced by PI3K, and interrupt AKT production to inhibit the PI3K-AKT pathway (*Kang, Lemke & Kim, 2009*). Thus, Pten is a primary regulator of the balance between survival and death in many cell lines, including vascular endothelial cells. Pten loss-of-function mutant mice exhibited enhanced activity of 3-phosphoinositide-dependent protein kinase and AKT (*Kurose et al., 2001*; *Stambolic et al., 1998*). In addition, Pten expression level was significantly increased in diabetic mouse aortas (*Takenouchi et al., 2008*). Our results proved that liraglutide reduced high-glucose-induced high expression of Pten. In addition to phosphorylating AKT, PI3K also regulates several other pathways, including the Bcl-2 pathway. Bcl-2 is a major anti-apoptotic protein that prevents cytochrome C release into the cytoplasm (*Do et al., 2015*; *Li et al., 1998*; *Luo et al., 1998*). miRNA mimic and inhibitor transfection demonstrated a negative correlation between miRNA-26a-5p and *Pten* expression. Moreover, we found that miR-181a-5p expression was decreased in the liraglutide-treated group. Creb is a miR-181a-5p target, and we also found that liraglutide treatment enhanced *Creb* expression in the aorta. In addition, miR-181a-5p expression is negatively correlated with *Creb* in vitro. Bcl-2 phosphorylation is followed by Creb serine-133 phosphorylation (*Das et al., 2005*). We found that liraglutide can reduce miR-34a-5p expression in vivo and in vitro.

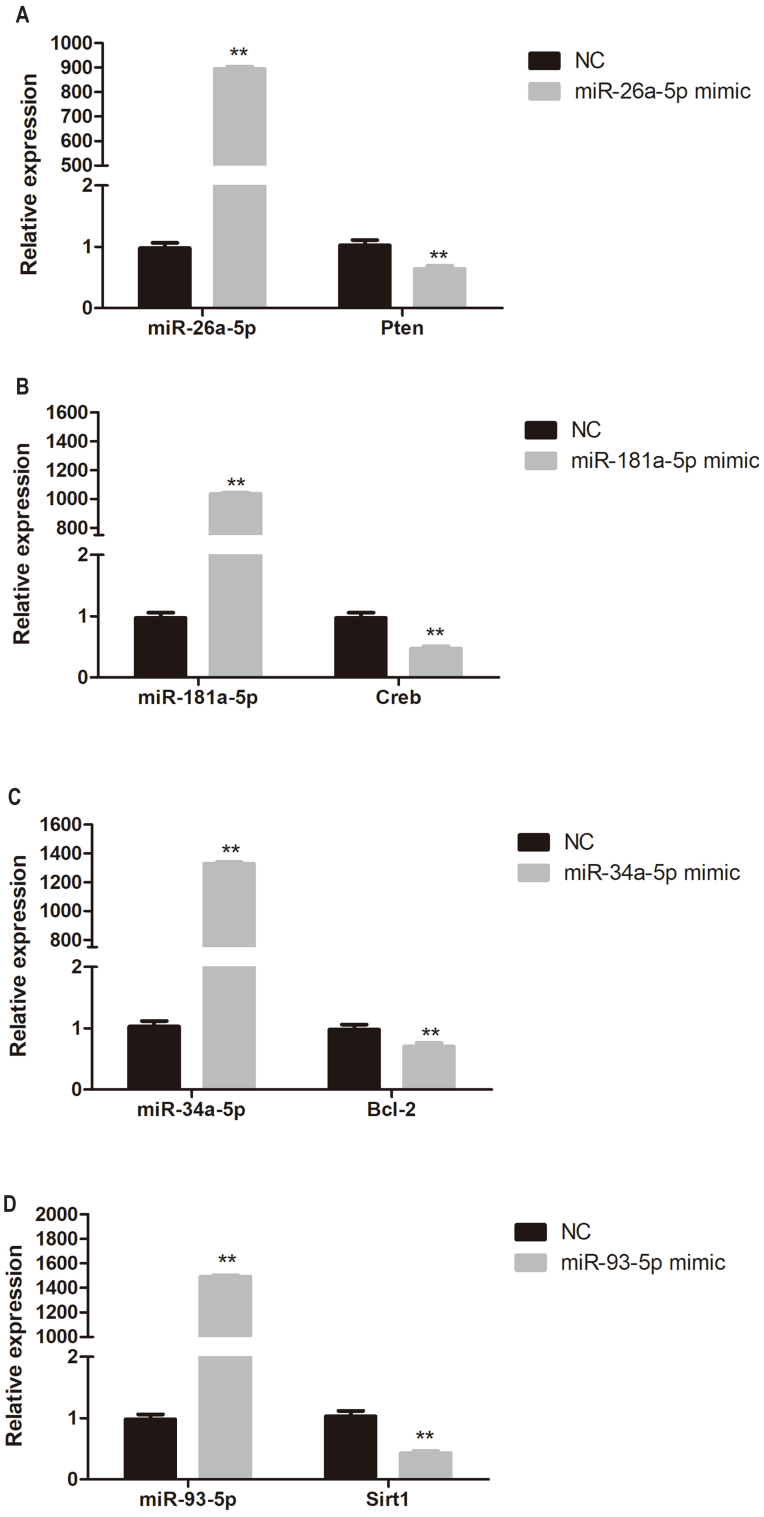

Figure 6 Quantitative PCR analysis of miR-26a-5p, miR-181a-5p, miR-34a-5p, miR-93-5p, *Pten*, *Creb*, *Bcl-2*, and *Sirt1* expression in miR-26a-5p (A), miR-181a-5p (B), miR-34a-5p (C), miR-93-5p (D) mimic transfected HUVECs. Data were presented as mean ± standard deviation (n = 6). $^{**}P < 0.01$ vs the NC group. *Creb*, cAMP responsive element binding protein; NC, negative control; *Pten*, phosphatase and tensin homologue on chromosome 10; Sirt1, Sirtuin 1. Full-size DOI: 10.7717/peerj.6567/fig-6

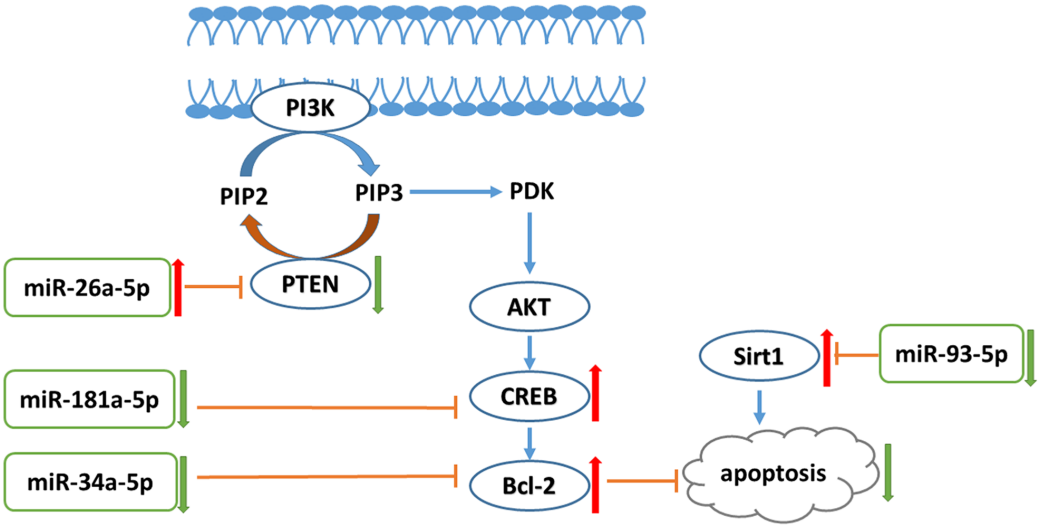

Figure 7 PI3K/AKT-Bcl-2 pathway was involved in the liraglutide treated aorta. Liraglutide increases miR-26a-5p to reduce PTEN thus increasing the levels of PIP3 to stimulate the PI3K-activated signaling cascades. In addition, liraglutide reduces miR-181a-5p and miR-34a-5p to increase the expression of Creb and Bcl-2, thus inhibiting the cell apoptosis. PTEN, phosphatase and tensin homologue on chromosome 10; PI3K, phosphoinositide 3-kinase; PIP2, phosphatidylinositol 4,5-bisphophate; PIP3, phosphatidylinositol (3,4,5)-trisphosphate; PDK, phosphoinositide-dependent kinase-1; Akt, serine/threonine kinase 1; Creb, cAMP responsive element binding protein; Sirt1, Sirtuin 1.

Full-size DOI: 10.7717/peerj.6567/fig-7

Inhibition of the miR-34 family by locked nucleic acid-modified antimiR improved systolic function in mice with impaired pathology and function (*Bernardo et al., 2012*). Bcl-2 is a miR-34a-5p target gene. We further found that *Bcl-2* expression was higher in the liraglutide-treated group than in the diabetes group and that miR-34a-5p and Bcl-2 expression levels were negatively correlated. High glucose levels reduced anti-apoptotic Bcl-2 expression in endothelial cells (*Qin et al., 2016*). Our result suggests that liraglutide increased Bcl-2 expression in high-glucose exposed HUVECs. Previous studies have shown that antioxidants can activate the Bcl-2 protein to inhibit INS-1 cell apoptosis (*Zheng et al., 2015*). A previous study found that exendin-4 increases Bcl-2 protein levels in tert-butyl hydroperoxide-treated HUVECs (*Wang et al., 2016*). Thus, our study showed that the PI3K-AKT signaling pathway was involved in the anti-apoptotic effects of liraglutide in endothelial cells.

Moreover, we found that liraglutide inhibited miR-93-5p expression in diabetic rat aortas. Sirtuin 1 (Sirt1) is target of miR-93-5p (*Li et al., 2011*) and we found that the expression of Sirt1 increased in liraglutide-treated rat aorta. miRNA mimic transfection revealed that miR-93-5p expression is negatively related to Sirt1 expression in HUVECs. SIRT1 is a type of NAD^+-dependent histone deacetylase and has various functions in inflammation, aging, and apoptosis (*Caito et al., 2010*). Sirt1 contributes to vascular protection through the deacetylation of several targets, including FOXO3 (*Hwang et al., 2013*) and p53 (*Nadtochiy et al., 2011*). Sirt1 has been previously recognized to protect endothelial cells against hyperglycemia-induced oxidative stress (*Kumar et al., 2017*) and

apoptosis (*Wang et al., 2017*). Our study demonstrated that liraglutide inhibits miR-93-5p, activating Sirt1 expression to protect endothelial cell function.

CONCLUSION

In conclusion, liraglutide can attenuate endothelial dysfunction. Liraglutide activates miR-26a-5p expression and inhibits miR-181a-5p, miR-34a-5p, and miR-93-5p expression in the aorta to inhibit endothelial cell apoptosis through the PI3K-AKT-Bcl-2 activation pathway (Fig. 7). In addition to the transcriptome, these results may provide attractive therapeutic options for targeting the epigenetic mechanisms of endothelial dysfunction via miRNAs.

ACKNOWLEDGEMENTS

We are very grateful to Beijing Compass Biotechnology Company for excellent technical assistance with the microarray experiments.

ADDITIONAL INFORMATION AND DECLARATIONS

Funding

This work was supported by grants from the National Key R&D Program of China (2017YFC1309603), the National Key Research and Development Program of China (2016YFA0101002), the Medical Epigenetics Research Center, the Chinese Academy of Medical Sciences (2017PT31036, 2018PT31021), the Non-profit Central Research Institute Fund of Chinese Academy of Medical Sciences (No. 2017PT32020, No. 2018PT32001), the National Natural Science Foundation of China (No. 81170736, 81570715, 81870579, 81870545), the National Natural Science Foundation for Young Scholars of China (No. 81300649), the China Scholarship Council foundation (201308110443), the PUMC Youth Fund (33320140022) and the Fundamental Research Funds for the Central Universities, and Scientific Activities Foundation for Selected Returned Overseas Professionals of Human Resources and Social Security Ministry. The funders had no role in study design, data collection and analysis, decision to publish, or preparation of the manuscript.

Grant Disclosures

The following grant information was disclosed by the authors:
National Key R&D Program of China: 2017YFC1309603.
National Key Research and Development Program of China: 2016YFA0101002.
Medical Epigenetics Research Center, Chinese Academy of Medical Sciences: 2017PT31036, 2018PT31021.
Non-profit Central Research Institute Fund of Chinese Academy of Medical Sciences: 2017PT32020, 2018PT32001.
National Natural Science Foundation of China: 81170736, 81570715, 81870579, 81870545.
National Natural Science Foundation for Young Scholars of China: 81300649.
China Scholarship Council foundation: 201308110443.

PUMC Youth Fund: 33320140022.
Fundamental Research Funds for the Central Universities, and Scientific Activities Foundation for Selected Returned Overseas Professionals of Human Resources and Social Security Ministry.

Competing Interests

The authors declare that they have no competing interests.

Author Contributions

- Qian Zhang conceived and designed the experiments, performed the experiments, prepared figures and/or tables, authored or reviewed drafts of the paper, approved the final draft.
- Xinhua Xiao conceived and designed the experiments, contributed reagents/materials/analysis tools, authored or reviewed drafts of the paper, approved the final draft.
- Jia Zheng performed the experiments.
- Ming Li analyzed the data.

Animal Ethics

The following information was supplied relating to ethical approvals (i.e., approving body and any reference numbers):

All procedures were performed in accordance with the Guide for the Care and Use of Laboratory Animals published by the U.S. National Institutes of Health (NIH publication No. 85-23, revised 1996) and were approved by the Animal Care Committee of the Peking Union Medical Hospital Animal Ethics Committee (Project XHDW-2015-0051, 15 Feb 2015).

Microarray Data Deposition

The following information was supplied regarding the deposition of microarray data:

The microarray raw data were submitted to the Gene Expression Omnibus (GEO) repository (GSE102198).

Data Availability

The following information was supplied regarding data availability:

The raw measurements are available in File S1.

Supplemental Information

Supplemental information for this article can be found online at http://dx.doi.org/10.7717/peerj.6567#supplemental-information.

REFERENCES

Andrikopoulos S, Blair AR, Deluca N, Fam BC, Proietto J. 2008. Evaluating the glucose tolerance test in mice. *American Journal of Physiology-Endocrinology and Metabolism* **295(6)**:E1323–E1332 DOI 10.1152/ajpendo.90617.2008.

Antunes LC, Elkfury JL, Jornada MN, Foletto KC, Bertoluci MC. 2016. Validation of HOMA-IR in a model of insulin-resistance induced by a high-fat diet in Wistar rats. *Archives of Endocrinology and Metabolism* **60(2)**:138–142 DOI 10.1590/2359-3997000000169.

Bangshaab M, Gutierrez A, Huynh KD, Knudsen JS, Arcanjo DDR, Petersen AG, Rungby J, Gejl M, Simonsen U. 2018. Different mechanisms involved in liraglutide and glucagon-like peptide-1 vasodilatation in rat mesenteric small arteries. *British Journal of Pharmacology* **176(3)**:386–399 DOI 10.1111/bph.14534.

Bao W, Aravindhan K, Alsaid H, Chendrimada T, Szapacs M, Citerone DR, Harpel MR, Willette RN, Lepore JJ, Jucker BM. 2011. Albiglutide, a long lasting glucagon-like peptide-1 analog, protects the rat heart against ischemia/reperfusion injury: evidence for improving cardiac metabolic efficiency. *PLOS ONE* **6(8)**:e23570 DOI 10.1371/journal.pone.0023570.

Bartel DP. 2004. MicroRNAs: genomics, biogenesis, mechanism, and function. *Cell* **116**:281–297.

Bernardo BC, Gao XM, Winbanks CE, Boey EJ, Tham YK, Kiriazis H, Gregorevic P, Obad S, Kauppinen S, Du XJ, Lin RC, McMullen JR. 2012. Therapeutic inhibition of the miR-34 family attenuates pathological cardiac remodeling and improves heart function. *Proceedings of the National Academy of Sciences of the United States of America* **109(43)**:17615–17620 DOI 10.1073/pnas.1206432109.

Bhashyam S, Fields AV, Patterson B, Testani JM, Chen L, Shen YT, Shannon RP. 2010. Glucagon-like peptide-1 increases myocardial glucose uptake via p38alpha MAP kinase-mediated, nitric oxide-dependent mechanisms in conscious dogs with dilated cardiomyopathy. *Circulation: Heart Failure* **3(4)**:512–521 DOI 10.1161/circheartfailure.109.900282.

Bonauer A, Carmona G, Iwasaki M, Mione M, Koyanagi M, Fischer A, Burchfield J, Fox H, Doebele C, Ohtani K, Chavakis E, Potente M, Tjwa M, Urbich C, Zeiher AM, Dimmeler S. 2009. MicroRNA-92a controls angiogenesis and functional recovery of ischemic tissues in mice. *Science* **324(5935)**:1710–1713 DOI 10.1126/science.1174381.

Caito S, Hwang JW, Chung S, Yao H, Sundar IK, Rahman I. 2010. PARP-1 inhibition does not restore oxidant-mediated reduction in SIRT1 activity. *Biochemical and Biophysical Research Communications* **392(3)**:264–270 DOI 10.1016/j.bbrc.2009.12.161.

Capes SE, Hunt D, Malmberg K, Gerstein HC. 2000. Stress hyperglycaemia and increased risk of death after myocardial infarction in patients with and without diabetes: a systematic overview. *Lancet* **355(9206)**:773–778 DOI 10.1016/S0140-6736(99)08415-9.

Chakravarthy U, Hayes RG, Stitt AW, McAuley E, Archer DB. 1998. Constitutive nitric oxide synthase expression in retinal vascular endothelial cells is suppressed by high glucose and advanced glycation end products. *Diabetes* **47(6)**:945–952 DOI 10.2337/diabetes.47.6.945.

Chou CH, Chang NW, Shrestha S, Hsu SD, Lin YL, Lee WH, Yang CD, Hong HC, Wei TY, Tu SJ, Tsai TR, Ho SY, Jian TY, Wu HY, Chen PR, Lin NC, Huang HT, Yang TL, Pai CY, Tai CS, Chen WL, Huang CY, Liu CC, Weng SL, Liao KW, Hsu WL, Huang HD. 2016. miRTarBase 2016: updates to the experimentally validated miRNA-target interactions database. *Nucleic Acids Research* **44(D1)**:D239–D247 DOI 10.1093/nar/gkv1258.

Das S, Cordis GA, Maulik N, Das DK. 2005. Pharmacological preconditioning with resveratrol: role of CREB-dependent Bcl-2 signaling via adenosine A3 receptor activation. *American Journal of Physiology-Heart and Circulatory Physiology* **288(1)**:H328–H335 DOI 10.1152/ajpheart.00453.2004.

Dennis G Jr, Sherman BT, Hosack DA, Yang J, Gao W, Lane HC, Lempicki RA. 2003. DAVID: database for annotation, visualization, and integrated discovery. *Genome Biology* **4**:P3.

Do M, Kim S, Seo SY, Yeo EJ, Kim SY. 2015. delta-Tocopherol prevents methylglyoxal-induced apoptosis by reducing ROS generation and inhibiting apoptotic signaling cascades in human umbilical vein endothelial cells. *Food & Function* **6(5)**:1568–1577 DOI 10.1039/c4fo01110d.

Fish JE, Santoro MM, Morton SU, Yu S, Yeh RF, Wythe JD, Ivey KN, Bruneau BG, Stainier DY, Srivastava D. 2008. miR-126 regulates angiogenic signaling and vascular integrity. *Developmental Cell* **15(2)**:272–284 DOI 10.1016/j.devcel.2008.07.008.

Gaspari T, Liu H, Welungoda I, Hu Y, Widdop RE, Knudsen LB, Simpson RW, Dear AE. 2011. A GLP-1 receptor agonist liraglutide inhibits endothelial cell dysfunction and vascular adhesion molecule expression in an ApoE$^{-/-}$ mouse model. *Diabetes and Vascular Disease Research* **8(2)**:117–124 DOI 10.1177/1479164111404257.

Hoang V, Bi J, Mohankumar SM, Vyas AK. 2015. Liraglutide improves hypertension and metabolic perturbation in a rat model of polycystic ovarian syndrome. *PLOS ONE* **10(5)**:e0126119 DOI 10.1371/journal.pone.0126119.

Hwang JW, Yao H, Caito S, Sundar IK, Rahman I. 2013. Redox regulation of SIRT1 in inflammation and cellular senescence. *Free Radical Biology and Medicine* **61**:95–110 DOI 10.1016/j.freeradbiomed.2013.03.015.

Islam MA, Akhtar MA, Khan MR, Hossain MS, Alam AH, Ibne-Wahed MI, Amran MS, Rahman BM, Ahmed M. 2009. Oral glucose tolerance test (OGTT) in normal control and glucose induced hyperglycemic rats with *Coccinia cordifolia* l. and *Catharanthus roseus* L. *Pakistan Journal of Pharmaceutical Sciences* **22**:402–404.

Ji R, Cheng Y, Yue J, Yang J, Liu X, Chen H, Dean DB, Zhang C. 2007. MicroRNA expression signature and antisense-mediated depletion reveal an essential role of MicroRNA in vascular neointimal lesion formation. *Circulation Research* **100(11)**:1579–1588 DOI 10.1161/CIRCRESAHA.106.141986.

Kang KH, Lemke G, Kim JW. 2009. The PI3K-PTEN tug-of-war, oxidative stress and retinal degeneration. *Trends in Molecular Medicine* **15(5)**:191–198 DOI 10.1016/j.molmed.2009.03.005.

Ke J, Liu Y, Yang J, Lu R, Tian Q, Hou W, Wang G, Wei R, Hong T. 2017. Synergistic effects of metformin with liraglutide against endothelial dysfunction through GLP-1 receptor and PKA signalling pathway. *Scientific Reports* **7(1)**:41085 DOI 10.1038/srep41085.

Kumar S, Kim YR, Vikram A, Naqvi A, Li Q, Kassan M, Kumar V, Bachschmid MM, Jacobs JS, Kumar A, Irani K. 2017. Sirtuin1-regulated lysine acetylation of p66Shc governs diabetes-induced vascular oxidative stress and endothelial dysfunction. *Proceedings of the National Academy of Sciences of the United States of America* **114(7)**:1714–1719 DOI 10.1073/pnas.1614112114.

Kurose K, Zhou XP, Araki T, Cannistra SA, Maher ER, Eng C. 2001. Frequent loss of PTEN expression is linked to elevated phosphorylated Akt levels, but not associated with p27 and cyclin D1 expression, in primary epithelial ovarian carcinomas. *American Journal of Pathology* **158(6)**:2097–2106 DOI 10.1016/s0002-9440(10)64681-0.

Larsen PJ, Wulff EM, Gotfredsen CF, Brand CL, Sturis J, Vrang N, Knudsen LB, Lykkegaard K. 2008. Combination of the insulin sensitizer, pioglitazone, and the long-acting GLP-1 human analog, liraglutide, exerts potent synergistic glucose-lowering efficacy in severely diabetic ZDF rats. *Diabetes, Obesity and Metabolism* **10(4)**:301–311 DOI 10.1111/j.1463-1326.2008.00865.x.

Latronico MV, Elia L, Condorelli G, Catalucci D. 2008. Heart failure: targeting transcriptional and post-transcriptional control mechanisms of hypertrophy for treatment. *International Journal of Biochemistry & Cell Biology* **40(9)**:1643–1648 DOI 10.1016/j.biocel.2008.03.002.

Li F, Ambrosini G, Chu EY, Plescia J, Tognin S, Marchisio PC, Altieri DC. 1998. Control of apoptosis and mitotic spindle checkpoint by survivin. *Nature* **396(6711)**:580–584 DOI 10.1038/25141.

Li J, Dong Y, Wu T, Tong N. 2016. Differences between Western and Asian type 2 diabetes patients in the incidence of vascular complications and mortality: a systematic review of randomized controlled trials on lowering blood glucose. *Journal of Diabetes* **8(6)**:824–833 DOI 10.1111/1753-0407.12361.

Li N, Muthusamy S, Liang R, Sarojini H, Wang E. 2011. Increased expression of miR-34a and miR-93 in rat liver during aging, and their impact on the expression of Mgst1 and Sirt1. *Mechanisms of Ageing and Development* **132(3)**:75–85 DOI 10.1016/j.mad.2010.12.004.

Luo X, Budihardjo I, Zou H, Slaughter C, Wang X. 1998. Bid, a Bcl2 interacting protein, mediates cytochrome c release from mitochondria in response to activation of cell surface death receptors. *Cell* **94(4)**:481–490 DOI 10.1016/s0092-8674(00)81589-5.

Malm-Erjefalt M, Bjornsdottir I, Vanggaard J, Helleberg H, Larsen U, Oosterhuis B, Van Lier JJ, Zdravkovic M, Olsen AK. 2010. Metabolism and excretion of the once-daily human glucagon-like peptide-1 analog liraglutide in healthy male subjects and its in vitro degradation by dipeptidyl peptidase IV and neutral endopeptidase. *Drug Metabolism and Disposition* **38(11)**:1944–1953 DOI 10.1124/dmd.110.034066.

Marso SP, Daniels GH, Brown-Frandsen K, Kristensen P, Mann JF, Nauck MA, Nissen SE, Pocock S, Poulter NR, Ravn LS, Steinberg WM, Stockner M, Zinman B, Bergenstal RM, Buse JB, Committee LS, Investigators LT. 2016. Liraglutide and cardiovascular outcomes in type 2 diabetes. *New England Journal of Medicine* **375(4)**:311–322 DOI 10.1056/NEJMoa1603827.

Matsumoto S, Shimabukuro M, Fukuda D, Soeki T, Yamakawa K, Masuzaki H, Sata M. 2014. Azilsartan, an angiotensin II type 1 receptor blocker, restores endothelial function by reducing vascular inflammation and by increasing the phosphorylation ratio Ser(1177)/Thr (497) of endothelial nitric oxide synthase in diabetic mice. *Cardiovascular Diabetology* **13(1)**:30 DOI 10.1186/1475-2840-13-30.

Nadtochiy SM, Redman E, Rahman I, Brookes PS. 2011. Lysine deacetylation in ischaemic preconditioning: the role of SIRT1. *Cardiovascular Research* **89(3)**:643–649 DOI 10.1093/cvr/cvq287.

Ogurtsova K, Da Rocha Fernandes JD, Huang Y, Linnenkamp U, Guariguata L, Cho NH, Cavan D, Shaw JE, Makaroff LE. 2017. IDF diabetes atlas: global estimates for the prevalence of diabetes for 2015 and 2040. *Diabetes Research and Clinical Practice* **128**:40–50 DOI 10.1016/j.diabres.2017.03.024.

Plamboeck A, Holst JJ, Carr RD, Deacon CF. 2005. Neutral endopeptidase 24.11 and dipeptidyl peptidase IV are both mediators of the degradation of glucagon-like peptide 1 in the anaesthetised pig. *Diabetologia* **48(9)**:1882–1890 DOI 10.1007/s00125-005-1847-7.

Plum A, Jensen LB, Kristensen JB. 2013. In vitro protein binding of liraglutide in human plasma determined by reiterated stepwise equilibrium dialysis. *Journal of Pharmaceutical Sciences* **102(8)**:2882–2888 DOI 10.1002/jps.23648.

Qin W, Ren B, Wang S, Liang S, He B, Shi X, Wang L, Liang J, Wu F. 2016. Apigenin and naringenin ameliorate PKCbetaII-associated endothelial dysfunction *via* regulating ROS/caspase-3 and NO pathway in endothelial cells exposed to high glucose. *Vascular Pharmacology* **85**:39–49 DOI 10.1016/j.vph.2016.07.006.

Quintavalle M, Condorelli G, Elia L. 2011. Arterial remodeling and atherosclerosis: miRNAs involvement. *Vascular Pharmacology* **55(4)**:106–110 DOI 10.1016/j.vph.2011.08.216.

Saeed AI, Bhagabati NK, Braisted JC, Liang W, Sharov V, Howe EA, Li J, Thiagarajan M, White JA, Quackenbush J. 2006. TM4 microarray software suite. *Methods in Enzymology* **411**:134–193 DOI 10.1016/S0076-6879(06)11009-5.

Skovso S. 2014. Modeling type 2 diabetes in rats using high fat diet and streptozotocin. *Journal of Diabetes Investigation* **5(4)**:349–358 DOI 10.1111/jdi.12235.

Stambolic V, Suzuki A, De La Pompa JL, Brothers GM, Mirtsos C, Sasaki T, Ruland J, Penninger JM, Siderovski DP, Mak TW. 1998. Negative regulation of PKB/Akt-dependent cell survival by the tumor suppressor PTEN. *Cell* **95(1)**:29–39 DOI 10.1016/s0092-8674(00)81780-8.

Sturis J, Gotfredsen CF, Romer J, Rolin B, Ribel U, Brand CL, Wilken M, Wassermann K, Deacon CF, Carr RD, Knudsen LB. 2003. GLP-1 derivative liraglutide in rats with beta-cell deficiencies: influence of metabolic state on beta-cell mass dynamics. *British Journal of Pharmacology* **140(1)**:123–132 DOI 10.1038/sj.bjp.0705397.

Su C, Xia T, Ren S, Qing S, Jing D, Lian H, Bin Q, Yuan Z, Xiang Z. 2014. Effect of diazoxide preconditioning on cultured rat myocardium microvascular endothelial cells against apoptosis and relation of PI3K/Akt pathway. *Balkan Medical Journal* **33(1)**:83–87 DOI 10.5152/balkanmedj.2013.8458.

Takenouchi Y, Kobayashi T, Matsumoto T, Kamata K. 2008. Possible involvement of Akt activity in endothelial dysfunction in type 2 diabetic mice. *Journal of Pharmacological Sciences* **106(4)**:600–608.

Wang S, Aurora AB, Johnson BA, Qi X, McAnally J, Hill JA, Richardson JA, Bassel-Duby R, Olson EN. 2008. The endothelial-specific microRNA miR-126 governs vascular integrity and angiogenesis. *Developmental Cell* **15(2)**:261–271 DOI 10.1016/j.devcel.2008.07.002.

Wang M, Li W, Chang GQ, Ye CS, Ou JS, Li XX, Liu Y, Cheang TY, Huang XL, Wang SM. 2011. MicroRNA-21 regulates vascular smooth muscle cell function via targeting tropomyosin 1 in arteriosclerosis obliterans of lower extremities. *Arteriosclerosis, Thrombosis, and Vascular Biology* **31(9)**:2044–2053 DOI 10.1161/ATVBAHA.111.229559.

Wang L, Tang L, Wang Y, Wang L, Liu X, Liu X, Chen Z, Liu L. 2016. Exendin-4 protects HUVECs from t-BHP-induced apoptosis via PI3K/Akt-Bcl-2-caspase-3 signaling. *Endocrine Research* **41(3)**:229–235 DOI 10.3109/07435800.2015.1110162.

Wang S, Wang J, Zhao A, Li J. 2017. SIRT1 activation inhibits hyperglycemia-induced apoptosis by reducing oxidative stress and mitochondrial dysfunction in human endothelial cells. *Molecular Medicine Reports* **16(3)**:3331–3338 DOI 10.3892/mmr.2017.7027.

Xie L, Wu Y, Fan Z, Liu Y, Zeng J. 2016. Astragalus polysaccharide protects human cardiac microvascular endothelial cells from hypoxia/reoxygenation injury: the role of PI3K/AKT, Bax/Bcl-2 and caspase-3. *Molecular Medicine Reports* **14(1)**:904–910 DOI 10.3892/mmr.2016.5296.

Yang Y, Fang H, Xu G, Zhen Y, Zhang Y, Tian J, Zhang D, Zhang G, Xu J. 2018. Liraglutide improves cognitive impairment via the AMPK and PI3K/Akt signaling pathways in type 2 diabetic rats. *Molecular Medicine Reports* **18(2)**:2449–2457 DOI 10.3892/mmr.2018.9180.

Zhang Q, Sun X, Xiao X, Zheng J, Li M, Yu M, Ping F, Wang Z, Qi C, Wang T, Wang X. 2016. Maternal chromium restriction leads to glucose metabolism imbalance in mice offspring through insulin signaling and Wnt signaling pathways. *International Journal of Molecular Sciences* **17(10)**:1767 DOI 10.3390/ijms17101767.

Zheng S, Zhao M, Ren Y, Wu Y, Yang J. 2015. Sesamin suppresses STZ induced INS-1 cell apoptosis through inhibition of NF-kappaB activation and regulation of Bcl-2 family protein expression. *European Journal of Pharmacology* **750**:52–58 DOI 10.1016/j.ejphar.2015.01.031.